ISBN: 978-3-95450-184-7 doi:10.18429/JACoW-IPAC2018-THPMK078

CORRUGATED STRUCTURE AS A LINEARIZER IN HIGH REPETITION RATE X-RAY FREE ELECTRON LASER SOURCE

Zhen Wang, Kaiqing Zhang, Chao Feng, Dazhang Huang, Meng Zhang
Shanghai Institute of Applied Physics, Chinese Academy of Sciences, Shanghai, China

Abstract

A feasible method is proposed to compensate the high order mode (HOM) of the RF field, linearize the bunch compression process in the high repetition rate x-ray free electron laser source. In the proposed scheme, the corrugated structure is used in the superconducting linac to linearize the longitudinal phase space of the electron beam. The results show that the peak current of the electron beam will be increased from about 1 kA to over 2 kA with the charge of 100 pC.

INTRODUCTION

Unlike the conventional lasers or the synchrotron radiation, the free-electron laser (FEL) [1] can generate the ultra-short, ultra-bright and fully-coherent hard x-ray radiation, which promotes FEL an impressive development in the last decade. Nowadays, many x-ray FEL facilities have been built or under-construction around the world, such as LCLS in the US [2], SACLA in Japan [3], FERMI in Italy [4, 5], Pal-FEL in Korea [6], SXFEL in China [7] and Swiss-FEL in Switzerland [8]. Since those facilities are driven by the normal conducting (copper) linac, the repetition rate of those facilities are 1-120 Hz, leading to a low average power.

Alternatively, high repetition rate FEL facilities based on superconducting technique have been studied for years. For example, FLASH [9] which is a soft x-ray user facility based on macro-bunch mode, has accumulated much experience on superconducting technique. Recently, the European-XFEL [10] successfully generates hard x-ray FEL, which is a milestone in the FEL community, and LCLS II in the US and SCLF in China being constructed are the hard x-ray FEL facilities based on superconducting linac and continue wave (CW) mode. The high repetition rates (about 1 MHz) FEL facilities could provide up to a thousand fold increase in average brightness compared with the normal conducting FEL facilities.

However, in order to provide the CW electron beam train, the normal conducting VHF RF gun [11] or the superconducting (SC) RF gun are adopted as the injector in the CW FEL facilities. The peak current of the electron beam at the end of the SC linac is only about 1kA, which is much lower than that of the normal conducting linac (about 3 kA). This leads to a degradation of the FEL performance. Much efforts and R&Ds have been made, mainly in the injector, to reduce the HOMs of the electron beam and to increase the peak current.

In this paper, we propose to use the corrugated structures to compensate the HOMs of the electron beam in the compression process. The corrugated structures are inserted upstream of the first bunch compressor chicane, providing strong wakefield to modulate the electron beam. The oscillation wavelength of the corrugated pipe wakefield is comparable to the duration and the HOMs wavelength of the electron beam at the entrance of the first bunch compressor chicane according to the theory and the simulation results. Three-dimension start-to-end simulations have been carried out to study the evolution of the longitudinal phase space and the comparison is made between the case with and without the corrugated pipe. The results show that the peak current of the electron beam at the end of the SC linac could achieve over 2 kA.

THEORY

A third harmonic cavity is used as the linearizer upstream of the first bunch compressor chicane (BC1) in the superconducting-linac-based high-repetition-rate FEL facilities. The Schematic layout of the gun, the linac segments and the first chicane are shown in Figure 1 with the symbols defined as voltage (V), RF phase (ϕ) and wavelength (λ) of each cryomodule in the injector (L0 CM) and the linac (L1 CM), as well as the chicane momentum compaction coefficients (R_{56}, T_{566}).

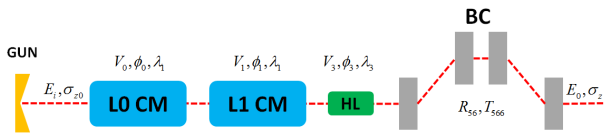

Figure 1: Schematic layout of the gun, the linac segments and the first chicane. The voltages and the phases in L0 CM are defined as the equivalent values V_0 and ϕ_0 for simplicity.

With initial energy E_i (at the end of the gun and buncher), and after passage through the accelerator RF systems, the electron energy at the first chicane is

$$E_0 \approx E_i + eV_0\cos(\phi_0 + k_1 z_0) + eV_1\cos(\phi_1 + k_1 z_0) + eV_3\cos(\phi_3 + k_3 z_0) \quad (1)$$

where $\phi_{0,1,3}$ and $V_{0,1,3}$ are the accelerating phases and voltages in each accelerating system, z_0 is the longitudinal position of the electron beam with respect to the reference particle, $k_{1,3} = \frac{2\pi}{\lambda_{1,3}}$ are the wavenumbers of the 1.3 GHz and 3.9 GHz superconducting RF cavities.

The energy deviation to the second-order in bunch length coordinate z_0 can be written as

ISBN: 978-3-95450-184-7 doi:10.18429/JACoW-IPAC2018-THPMK078

$$az_0+bz_0^2=\frac{\Delta E}{E_0}=\left(\frac{-eV_0k_1\sin\phi_0-eV_1k_1\sin\phi_1}{E_0}\right)z_0+\left(\frac{-eV_0k_1^2\cos\phi_0-eV_1k_1^2\cos\phi_1-eV_3k_3^2\cos\phi_3}{2E_0}\right)z_0^2 \quad (2)$$

The bunch length coordinate z, after the beam passing through the chicane, to second order is given as

$$z=z_0+R_{56}\cdot\frac{\Delta E}{E_0}+T_{566}\cdot\left(\frac{\Delta E}{E_0}\right)^2 \quad (3)$$

where $T_{566}\approx-\frac{3}{2}R_{56}$ is satisfied for a typical chicane.

Substitute equation (2) into equation (3), one has

$$z=\left(1+aR_{56}\right)z_0+\left(bR_{56}+a^2T_{566}\right)z_0^2 \quad (4)$$

Set the second term to zero to linearize the transformation, one have

$$bR_{56}+a^2T_{566}=0 \quad (5)$$

For the linear compression, one has the relation

$$-aR_{56}\approx1-\sigma_z/\sigma_{z_0} \quad (6)$$

Finally, one could have the necessary harmonic voltage as

$$eV_3\cos\phi_3=\frac{E_0\left[1-\frac{\lambda_1^2}{2\pi^2}\frac{T_{566}}{R_{56}^3}\left(1-\frac{\sigma_z}{\sigma_{z_0}}\right)^2\right]-E_i}{1-\left(\frac{\lambda_1}{\lambda_3}\right)^2} \quad (7)$$

The typical longitudinal phase space of the electron beam at the end of the SC linac is shown in Figure 2, in which one can see that the bunch-length-scale energy modulation leads to the double-horn density distribution and the peak current of the high-quality beam is about 1kA.

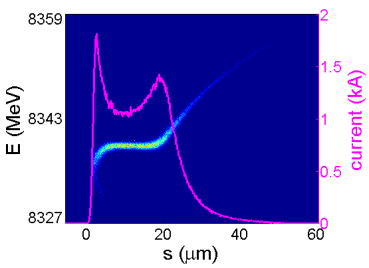

Figure 2: Longitudinal phase space of the electron beam at the exit of the linac. 's' is the coordinate along the beam and the bunch head is to the left.

The corrugated structures, is quite suitable to compensate the HOMs of the electron beam and linearize the energy chirp of the electron beam as the 'additional linearizer' [12]. The geometry of the corrugated structure is shown in Figure 3.

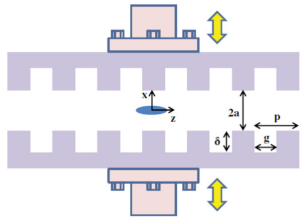

Figure 3: The geometry of the corrugated structure.

When the relativistic charged beam passes through the structure, a strong fundamental mode with a frequency that is far above the beam pipe cut-off is excited. The longitudinal point charge wake is approximately given by

$$W(s)=2\chi H(s)\cos ks \quad (8)$$

The χ is the mode loss factor by

$$\chi=\frac{Z_0c}{2\pi a^2} \quad (9)$$

where $Z_0=377\Omega$ represents the characteristic impedance of vacuum and c is the speed of light.

The $H(s)$ is the unit step function with

$$H(s)=\begin{cases}1, s\geq0\\0, s<0\end{cases} \quad (10)$$

and the wave number, k, is well approximated by

$$k=\sqrt{\frac{2p}{a\delta g}} \quad (11)$$

For a bunch with longitudinal distribution $\lambda(s)$, the bunch wake is given by the convolution

$$W_\lambda(s)=-\int_0^{+\infty}W(s')\lambda(s-s')ds' \quad (12)$$

Considering a Gaussian bunch density distribution beam with the bunch length of σ_z without any current fluctuation. We choose the wavelength of the point charge wake approximately equal to the bunch length and carry out the calculation of the field within the beam for simplification. The results are shown in Figure 4.

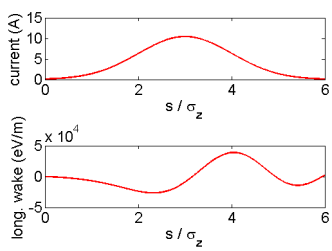

Figure 4: the Gaussian bunch and the longitudinal wake along the bunch.

3D SIMULATIONS

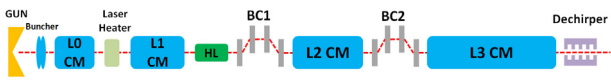

Figure 5: the scheme layout of the injector and the linac of SCLF.

ISBN: 978-3-95450-184-7 doi:10.18429/JACoW-IPAC2018-THPMK078

The Shanghai Coherent Light Facility (SCLF) will be the first hard x-ray FEL user facility based on superconducting linac technique in China. The layout of the injector and the linac of the SCLF are shown in Figure 5. The main parameters of the SCLF are listed in Table 1.

Table 1: The Main Parameters of the SCLF

Energy (GeV)	8
Slice energy spread (rms)	<0.01%
Normalized slice emittance (mm mrad)	<0.4
Charge (pC)	100
Repetition rate (MHz)	1
Peak current (kA)	1
Bunch length (um, rms)	8
Transverse beam size (um, rms)	30

In order to illustrate the beam dynamic of the bunch, three-dimensional simulations were carried out with all components of the SCLF. The injector simulations were accomplished using the computer tracking codes ASTRA [13] with the space charge effects taking into account. The linac simulations were carried out using ELEGANT [14] including the coherent synchrotron radiation effects (CSR) and longitudinal wakefield. The longitudinal phase space evolution of the electron beam along the beamline are given in Figure 6. Based on Figure 6 it is clear to see that the peak current of the high-quality part of the electron beam is only about 1 kA and the double-horn-like current distribution limits the higher peak current because of the HOMs of the electron beam.

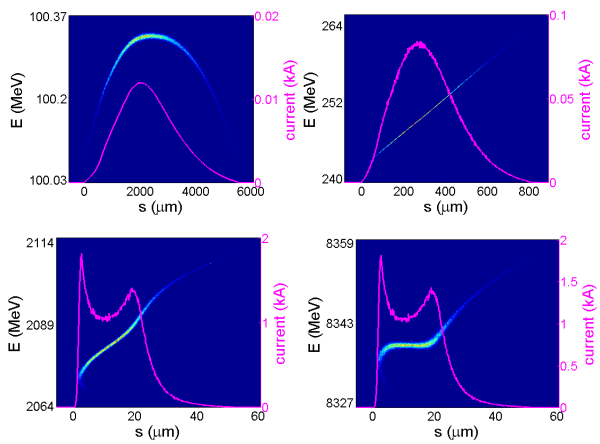

Figure 6: Longitudinal phase space of the electron beam along the beamline at the exit of (top left) the injector; (top right) the BC1; (bottom left) the BC2 and (bottom right) the linac.

In order to compensate the HOMs of the beam, three dimensional simulations (with LiTrack and ELEGANT) were carried out to analyze the longitudinal phase space evolution of the electron beam based on the SCLF. In our simulations, a 0.4m-long corrugated pipe with the parameters in Table 2 is inserted downstream of the 3.9 GHz third harmonic cavities in L1 in order to compensate the HOMs of the electron beam. The longitudinal phase space, beam current and slice energy spread distribution at the exit of the linac are summarized in Figure 7, in which one can find that the electron beam maintains high quality in an approximately 50 fs wide with current over 2 kA, slice energy spread of 800 keV and normalized slice emittance of 0.25 mm mrad.

Table 2: Main Parameters of the Corrugated Structure

Parameters	Values 1	Values 2	Units
Radius a	2.5	1.0	mm
Period p	1.0	0.3	mm
Depth δ	0.4	0.3	mm
Width g	0.2	0.2	mm
Length L	0.4	0.06	m

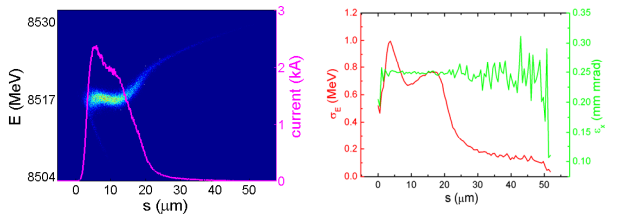

Figure 7: (left) Longitudinal phase space of the electron beam; (right) beam current and slice energy spread distribution.

CONCLUSIONS

Due to strong space charge effects, the peak current of the electron beam is limited to about 1 kA in high-repetition-rate free electron laser light source. In order to improve the peak current, the corrugated structure is proposed to be employed as the 'additional linearizer' downstream of the third harmonic cavity to compensate the HOM of the electron beam during the compression process. The optimal parameters of the corrugated structures are given in the article and the simulation results show that the 'additional linearizer' works well. One can compress the beam further to higher peak current, e.g., over 2 kA in our simulations, which improves the FEL performance very much.

ISBN: 978-3-95450-184-7 doi:10.18429/JACoW-IPAC2018-THPMK078

REFERENCES

[1] J. M. J. Madey, Stimulated Emission of Bremsstrahlung in a Periodic Magnetic Field, *Journal of Applied Physics*,vol. 42 (1971) 1906.

[2] P. Emma *et al*., First lasing and operation of an ångstrom-wavelength free-electron laser, *Nat. Photonics*, vol. 4, 641 (2010).

[3] H. Tanaka *et al*., A compact X-ray free-electron laser emitting in the sub-ångstrom region, *Nat. Photonics* vol. 6, 540 (2012).

[4] E. Allaria *et al*., Highly coherent and stable pulses from the FERMI seeded free-electron laser in the extreme ultraviolet, *Nat. Photonics*,vol.6, 699 (2012).

[5] E. Allaria *et al*., Two-stage seeded soft-X-ray free-electron laser, *Nat. Photonics*, vol. 7, 913 (2013).

[6] H. Kang et al., Hard X-ray free-electron laser with femtosecond-scale timing jitter, *Nat. Photonics*, vol. 11, 708 (2017).

[7] Z. T. Zhao *et al*., Shanghai soft x-ray free electron laser test facility, in *Proc. IPAC2011*, San Sebastián, Spain, THPC053.

[8] B. D. Patterson *et al*., Coherent science at the SwissFEL x-ray laser, *New J. Phys.*, vol. 12, p. 035012 (2010).

[9] W. A. Ackermann *et al*., Operation of a free-electron laser from the extreme ultraviolet to the water window, *Nat. Photonics*, vol. 1, 336 (2007).

[10] R. Abela *et al*., XFEL: The European X-Ray Free-Electron Laser - Technical Design Report (DESY, Ham-burg, 2006), pp. 1-646.

[11] F. Zhou *et al*., LCLS-II injector physics design and beam tuning, in *Proc. IPAC2017*, Copenhagen, Denmark, TUPAB138.

[12] Q. Gu, M. Zhang and M. H. Zhao, A passive linearizer for bunch compression, in *Proc. LINAC2012*, Tel-Aviv, Israel, TUPB022.

[13] K. Floettmann, ASTRA User's Manual, available at ***http://www.desy.de/mpyflo/Astra_ dokumentationS***

[14] M. Borland, "Elegant: A flexible SDDS-compliant code for accelerator simulation", Advanced Photon Source Rep., No. LS-287, 2000